Available online at www.sciencedirect.com
ScienceDirect
Chemical Physics 343 (2008) 19–30
Chemical Physics
www.elsevier.com/locate/chemphys

High resolution electron momentum spectroscopy of the valence orbitals of water

C.G. Ning [a], B. Hajgató [b], Y.R. Huang [a,b], S.F. Zhang [a], K. Liu [a], Z.H. Luo [a], S. Knippenberg [b], J.K. Deng [a,*], M.S. Deleuze [b,*]

[a] Department of Physics and Key Laboratory of Atomic and Molecular NanoSciences of MOE, Tsinghua University, Beijing 100084, PR China
[b] Research Group of Theoretical Chemistry, Department SBG, Hasselt University, Agoralaan Gebouw D, B-3590 Diepenbeek, Belgium

Received 12 June 2007; accepted 17 September 2007
Available online 26 September 2007

Abstract

The development of a third-generation electron momentum spectrometer with significantly improved energy and momentum resolutions at Tsinghua University ($\Delta E = 0.45$–0.68 eV, $\Delta\theta = \pm 0.53°$ and $\Delta\phi = \pm 0.84°$) has enabled a reinvestigation of the valence orbital electron momentum distributions of H_2O with improved statistical accuracy. The measurements have been conducted at impact energies of 1200 eV and 2400 eV in order to check the validity of the plane wave impulse approximation. The obtained ionization spectra and electron momentum distributions have been compared with the results of computations carried out with Hartree Fock [HF] theory, density functional theory in conjunction with the standard B3LYP functional, one-particle Green's function [1p-GF] theory along with the third-order algebraic diagrammatic construction scheme [ADC(3)], symmetry adapted cluster configuration interaction [SAC-CI] theory, and a variety of multi-reference [MR-SDCI, MR-RSPT2, MR-RSPT3] theories. The influence of the basis set on the computed momentum distributions has been investigated further, using a variety of basis sets ranging from 6-31G to the almost complete d-aug-cc-pV6Z basis set. A main issue in the present work pertains to a shake-up band of very weak intensity at 27.1 eV, of which the related momentum distribution was analyzed for the first time. The experimental evidences and the most thorough theoretical calculations demonstrate that this band borrows its ionization intensity from the $2a_1$ orbital.

Keywords: Electron momentum spectroscopy; Green functions; SAC-CI; Water

1. Introduction

Electron momentum spectroscopy (EMS), also known as (e, 2e) spectroscopy, is a powerful tool for investigating the electronic structure of matter [1–4]. The basic principle of EMS is a kinematically complete study of electron impact ionization events inducing (e, 2e) reactions. The differential cross-sections at sufficiently high energies are very sensitive to the energy-momentum densities. The observed momentum distributions (MD) are most usually analyzed through comparisons with theoretical calculations performed under the assumptions of the Born–Oppenheimer, binary encounter, and plane wave impulse approximations (PWIA). Under the so-called EMS conditions associated with electron impact ionization events at high kinetic energies ($E_0 \gg 1$ keV), these approximations enable indeed a rather straightforward mapping between the experimentally obtained momentum distributions and the calculated orbital electron densities. EMS is therefore most commonly regarded as a powerful "orbital imaging" technique. It is justifiable to some extent to employ this technique for evaluating the reliability of theoretical wave functions with regards to the usual limitations encountered in molecular quantum mechanics, namely the size of the employed basis set, and the level achieved in treating electronic correlation

* Corresponding authors. Tel.: +86 10 6278 5594; fax: +86 10 6278 1604 (J.K. Deng); tel.: +32 11 26 83 03; fax: +32 11 26 83 11 (M.S. Deleuze).
E-mail addresses: djk-dmp@tsinghua.edu.cn (J.K. Deng), michael.deleuze@uhasselt.be (M.S. Deleuze).

0301-0104/$ - see front matter © 2007 Elsevier B.V. All rights reserved.
doi:10.1016/j.chemphys.2007.09.030

within the neutral ground state. However, the available EMS spectrometers still badly need improvements with regards to energy and momentum resolution for probing on more quantitative grounds the outcome of the dynamical correlation and relaxation effects induced by (e, 2e) ionization processes on the effective shape and spread of the orbitals involved in these processes. In an exact theory of ionization at the limit of high kinetic energies for the impinging electrons, the measured electron momentum distributions relate to Dyson orbitals [5–12], measuring partial overlaps between the neutral ground state and the corresponding cationic states of the target.

Various experimental and theoretical investigations have been reported to date on the electronic states of water, and interest in this tremendously important molecule in chemistry, biology, physics, geology, hydrology, etc. remains unabated [13–27]. The first reported studies using EMS were early works by Dixon et al. [28] and Hood et al. [29]. Subsequent works by Bawagan et al. [30,31] have extensively investigated the electronic states of water using EMS methods. In these works, a comparison with results obtained from configuration interaction (CI) calculations has enlightened the importance of the electron correlation effects in describing the low momentum parts of outer valence electron distributions. However, a major drawback in these early experimental studies is the low statistical accuracy, which impeded the identification of weak satellite states at experimental ionization energies around 27 eV. Also, these states were not recovered by the theoretical calculations presented in the work by Bawagan et al. [31] with an even tempered set of 109 Gaussian Type Orbital (GTO's) basis functions. However, shake-up states with exceedingly limited strength and with the appropriate symmetry could be recovered nearly four decades ago at ~27 eV from very simple Green's Function calculations of the ionization spectrum of water [32], using an expansion of the self-energy that is correct through second-order and incorporates partial infinite series of higher-order terms by virtue of a renormalization of the energy denominators. Although of weak intensity, a shake-up band was also very clearly discernable at 27 eV in the valence electronic spectroscopy for chemical analysis (ESCA) spectrum of water recorded by Siegbahn et al., also more than four decades ago [33]. This exceedingly challenging issue was nonetheless most commonly eluded in later theoretical investigations of the ionization spectrum of water [34–51]. The existence of these shake-up states has received recently strong support, both experimentally and theoretically, from high resolution synchrotron radiation PES measurements [52], and calculations employing the symmetry adapted cluster configuration interaction (SAC-CI) scheme at the level of the general-R approximation [53]. It is thus now almost 20 years that the pioneering EMS work by Bawagan et al. [31] on water is awaiting a confirmation on more robust experimental grounds of the momentum profiles associated to the shake-up ionization channels of water.

In the present work, we report therefore a new experimental EMS investigation, at higher resolution and statistical accuracy, of the momentum distributions associated to all valence orbitals of water, throughout the valence region, up to electron binding energies of ~45 eV. This study has been made possible by the development of an electron momentum spectrometer of the third generation at Tsinghua University. The azimuthal and polar angular resolutions, and energy resolutions that are achieved at present under (e, 2e) non-coplanar symmetric kinematics are $\Delta\phi = \pm 0.84°$, $\Delta\theta = \pm 0.53°$, and $\Delta E = 0.45$–0.68 eV (depending on the electron beam current), respectively. Further theoretical calculations employing a variety of single-reference and multi-reference quantum mechanical methods are performed for elucidating the origin of the shake-up band at 27 eV.

2. Theory and computational details

EMS is a binary (e, 2e) experiment in which an incident electron with high enough energy E_0 induces ionization of a molecular target. The scattered and ionized electrons are subsequently detected in coincidence at equal kinetic energies and equal polar angles, i.e. $E_1 \approx E_2$, and $\theta_1 = \theta_2 = 45°$. The initial momentum p of the knocked-out electron obeys therefore a simple conservation rule:

$$p = \left\{ (2p_1 \cos\theta_1 - p_0)^2 + [2p_1 \sin\theta_1 \sin(\phi/2)]^2 \right\}^{1/2}, \qquad (1)$$

where p_1, p_2 ($p_1 \approx p_2$) are the momentum of each of the two outgoing electron, and p_0 is the momentum of the incident electron.

Under the assumptions of the Born (sudden or vertical), binary encounter, and plane wave impulse approximations (PWIA), the triple differential EMS cross-section for randomly oriented molecules is then given by

$$\sigma_{\mathrm{EMS}} \propto \int \mathrm{d}\Omega \left| \left\langle \upsilon_{\vec{p}} \Psi_f^{N-1} | \Psi_i^N \right\rangle \right|^2, \qquad (2)$$

where $\upsilon_{\vec{p}}$ represents a plane wave function $e^{i\vec{p}\cdot\vec{r}}$. The overlap of the ion and neutral wavefunctions in Eq. (2) is referred to as a Dyson orbital [5–12]. Dyson orbitals are straightforwardly obtained from CI [31] or Green's Function (GF) calculations [9–11,54]. Assuming a depiction of ionization events at the level of Koopmans' theorem, Dyson orbitals most naturally reduce to Hartree–Fock orbitals (Target Hartree–Fock Approximation, THFA) with a spectroscopic strength equal to 1. Most EMS experiments nowadays are interpreted using the empirical Target Kohn–Sham Approximation (TKSA), which amounts to substituting Dyson orbitals by the most relevant Kohn–Sham orbitals. With the THFA or TKSA, and upon accounting for the dispersion of the ionization intensity over shake-up and shake-off satellites, Eq. (2) then simply becomes [55,56]

$$\sigma_{\mathrm{EMS}} \propto S_i^f \int \mathrm{d}\Omega |\psi_i(p)|^2, \tag{3}$$

where $\psi_i(p)$ represents the momentum space representation, i.e. Fourier transform, of a canonical HF or KS orbital, and S_i^f denotes the associated pole strength. Neutral ground state correlation is by construction included in the Kohn–Sham orbital through the exchange-correlation potential [56]. In contrast, many-body effects in the final state are very obviously not accounted for by these orbitals in standard applications of density functional theory. In the present work, we therefore comparatively study the outcome of DFT calculations using the standard hybrid Becke-Perdew-3-parameters-Lee-Yang-Parr (B3LYP) functional [57] with more reliable Dyson orbital calculations of electron momentum distributions. To investigate further the influence of the basis set, a new program (NEMS) has been implemented for computing HF and KS momentum distributions using an almost complete basis set, namely d-aug-cc-pV6Z [58]. The neutral molecular equilibrium geometry ($R_{\mathrm{OH}} = 0.9572$ Å, $\theta_{\mathrm{HOH}} = 104.52°$) was used for generating the calculated wave functions [31].

As EMS, 1p-GF theory enables a direct mapping, and this within an exact many-body framework, of vertical ionization energies and Dyson orbitals. In its energy representation, the advanced (A) component of the one-particle Green's Function (1p-GF) has indeed the following definition [12]:

$$G^A(\mathbf{x}_2, \mathbf{x}_1, \omega) = \sum_f \frac{g_f(\mathbf{x}_2) g_f^*(\mathbf{x}_1)}{\omega - (E_0^N - E_f^{N-1}) - i0^+}, \tag{4}$$

where the sum over f runs over all the electronic configurations of the molecular radical cation M^+. It is immediately apparent that the poles of this component of the 1p-GF give access to ionization energies, whereas the corresponding residues relate to products of Dyson orbitals and to ionization intensities therefore [12].

Employing the formalism of second quantization, Dyson orbitals can be expanded as linear combinations of canonical (i.e. orthonormal) occupied and unoccupied HF orbitals, $\phi_i(\mathbf{x})$, with Feynman–Dyson transition amplitudes, X_{fi}, as weight coefficients:

$$g_f(\mathbf{x}) = \sum_i \phi_i(\mathbf{x}) \left\langle \Psi_f^{N-1} | a_i | \Psi_0^N \right\rangle = \sum_i X_{fi} \phi_i(\mathbf{x}). \tag{5}$$

The norms, Γ_f, of Dyson orbitals define spectroscopic pole strengths [12], which provide a straightforward estimate of relative ionization intensities [59], regardless of cross-section effects

$$\Gamma_f = \sum_i |X_{fi}|^2. \tag{6}$$

At the ADC(3) level, one-electron and shake-up ionization energies are obtained as eigenvalues (E) of a secular matrix ($\mathbf{H}$) cast over the one-hole (1h) and two-hole/one-particle (2h-1p) excited (shake-up) configurations of the radical cation M^+, as well as 1p and 2p-1h (shake-on) anionic configurations produced by electron attachment processes on M [60–62]. The sets of Feynman–Dyson transition amplitudes ($\{X_{fi}\}$) required to expand Dyson orbitals derive [12,63] from the 1h and 1p components of the associated eigenvectors ($\mathbf{HX} = \mathbf{XE}$, $\mathbf{X}^\dagger\mathbf{X} = \mathbf{1}$). By virtue of its treatment of static and dynamic self-energies, through fourth- and third-order in correlation [54], respectively, the 1p-GF/ADC(3) approach predicts vertical one-electron ionization energies within accuracies of ~0.2 eV [64,65]. In contrast with comparable MR-SDCI (multi-reference single and double CI) treatments, the 1p-GF/ADC(3) scheme is size-consistent [66] and applicable therefore to extremely large systems [67]. Unlike DFT calculations employing standard functionals, a charge-consistent ADC(3) scheme guarantees that the associated scattering potentials have the correct scaling in the asymptotic region [66]. A drawback of the ADC(3) scheme is the limited order attained in correlation for the shake-up energies. Whereas one-electron ionization energies are treated through third-order, singly-excited 2h-1p shake-up states are of first-order only, and higher-rank (double, triple, etc.) electronic excitations are neglected. An ADC(3) treatment of shake-up states is therefore comparable with a CIS calculation of excited states in molecular radical cations. Nonetheless, in most applications of the ADC(3) approach, the achieved accuracy on 2h-1p shake-up ionization energies ranges usually from ~0.5 to ~1 eV, depending on the energy of the ionized orbital (see Ref. [9] and references therein).

Recent SAC-CI general R calculations using a cc-pVTZ basis set augmented by $\alpha_s = 0.059$, 0.017, 0.0066; $\alpha_p = 0.059$, 0.015, 0.0054; $\alpha_d = 0.059$, 0.016, 0.0032 Rydberg functions [68] on the oxygen atom (from now on abbreviated to rTZ) appeared to be required for reproducing the $2a_1$ shake-up states of water at ~27.1 eV [53]. The symmetry adapted cluster configuration interaction (SAC-CI) general-R method [69] is designed to describe multiple-electron processes with extremely high accuracy because it involves single, double, and higher excitation operators up to sextuple excitations. The SAC-CI general-R approach has also been amply used for studying congested ionization spectra and is especially powerful for shake-up states [69–71]. Remembering that most theoretical works so far on the ionization spectrum of water failed to reproduce the shake-up states at ~27.1 eV, we believe that a comparison of further improved SAC-CI calculations with other many-body quantum mechanical calculations might be useful. One may indeed wonder whether the failure of many previous theoretical studies in describing the $2a_1$ shake-up states of water at ~27.1 eV is ascribable to the lack of Rydberg atomic functions in the employed basis sets, which are most reasonably expected to be essential for calculating shake-up states when these states fall in energy ranges similar to the valence electron binding energies. In the present work, the ionization spectrum of water is therefore investigated further using a variety of methods employing an even larger basis set than the one used by Ehara et al. [53]. More specifically, in our work, use was

made of a Rydberg augmented Triple Zeta (raTZ) basis set derived from Dunning's aug-cc-pVTZ basis set [72], which has been augmented with s-, p-, and d-type Rydberg functions for O atom: $\alpha_s = 0.017,\ 0.0066$; $\alpha_p = 0.015,\ 0.0054$; $\alpha_d = 0.059,\ 0.016,\ 0.0032$ [68]. Our raTZ basis set therefore incorporates in total 115 basis functions, compared with the 85 functions in the basis set used by Ehara et al. [53]. For comparison purposes, besides these SAC-CI general R/raTZ calculations, we also provide the results of ADC(3)/raTZ calculations. In the present work, all single-reference calculations were performed at Hasselt University using the Gaussian03 [73] program package [SAC-CI], except the ADC(3) calculations that were carried out using the original package of programs by Schirmer, Cederbaum and co-workers [60–62]. In the latter calculations, the retained threshold on pole strengths in the final block-Davidson diagonalization procedure was 0.001.

Comparison is further made with the results of calculations of the excited states of the water radical cation (H_2O^+) employing multi-reference single and double configuration interaction theory (MR-SDCI) [74–76]. In our work, these calculations are based on CAS reference wave functions employing an active space constructed by distributing the 7 valence electrons over 11 orbitals, among which there are 6, 3, and 2 orbitals with a_1, b_1 and b_2 symmetry labels, respectively [CAS(7,11)]. The same wavefunction was used to carry our further multi-reference calculations in conjunction with second- and third-order Rayleigh Schrödinger perturbation theory (MR-RSPT2; MR-RSPT3 [77]). All these multi-reference calculations have been performed at Hasselt University using the Molpro2000 package [78].

3. Experimental set up

Recently, a high sensitivity EMS spectrometer was constructed at Tsinghua University (THU), which features a high coincidental count-rate [79]. It exploits symmetric non-coplanar conditions and uses a double toroidal energy analyzer and position sensitive detectors to achieve the energy and angle multi-channel detection. Although its coincidental count rate is about two orders of magnitude higher than that of our previous spectrometer, the resolution has not been improved yet. To achieve higher resolutions, significant modifications have been implemented on this spectrometer. Briefly, an electron gun equipped with the oxide cathode, which worked at a much lower temperature than the generic filament cathodes, is used to generate the electron beam with low energy spread and low divergence angle. The electron beam size is constrained to 0.3 mm in diameter by a molybdenum aperture and the pass energy is set to 50 eV for improving the momentum resolution and energy resolution. Since the oxide cathode is easily poisoned by active gas, an additional vacuum chamber has been designed to mount the electron gun, which is evacuated to a base pressure 10^{-7} Pa by a 600 L/s molecular turbopump, which has a 2 mm diameter hole connect to the main chamber for electron beam passing through. With these measures and optimization of electron optics using the Monte Carlo simulation, the angle resolutions which were $\Delta\phi = \pm 0.84°$, $\Delta\theta = \pm 0.53°$, respectively, were obtained by standard calibration run for argon. The ratio of peak to valley for the argon 3p momentum distribution reached 8.5:1 at an impact energy of 1200 eV plus binding energy. The achieved momentum resolution is $\Delta p \sim 0.16$ a.u. (FWHM) or $\Delta p = 0.069$ a.u. (one standard deviation) at an impact energy (E_0) of 1200 eV. At $E_0 = 2400$ eV, Δp is correspondingly around 0.23 a.u. (FWHM) or $\Delta p = \pm 0.098$ a.u. (one standard deviation). The energy resolution is highly dependent on the emitting current of the cathode due to the space charge effects. The energy resolution $\Delta E = 0.45$ eV (FWHM) is obtained with an emitting current of 1 μA at an impact energy 1200 eV. This resolution deteriorates to $\Delta E = 0.68$ eV (FWHM) with an emitting current of 6 μA. Compared with the resolution $\Delta E = 1.6$ eV FWHM achieved previously by Bawagan et al. [31], an energy resolution of $\Delta E = 0.68$ eV (FWHM) is still good enough for improving in details the experimental EMS characterization of water. The electron gun has therefore been operated at a constant emitting current of 6 μA for shortening the measuring period. The collected current in the Faraday cup which is placed after the reaction region is only about 16% of the cathodic current, due to an aperture of 0.3 mm. Despite this loss of intensity for the impinging electron beam, the typical coincidental count rate is ~12 per second at an impact energy of 1200 eV in EMS experiments on an argon sample.

4. Results and discussion

4.1. Density map

Fig. 1 shows the momentum-energy density map of H_2O at an electron impact energy of 1200 eV plus binding

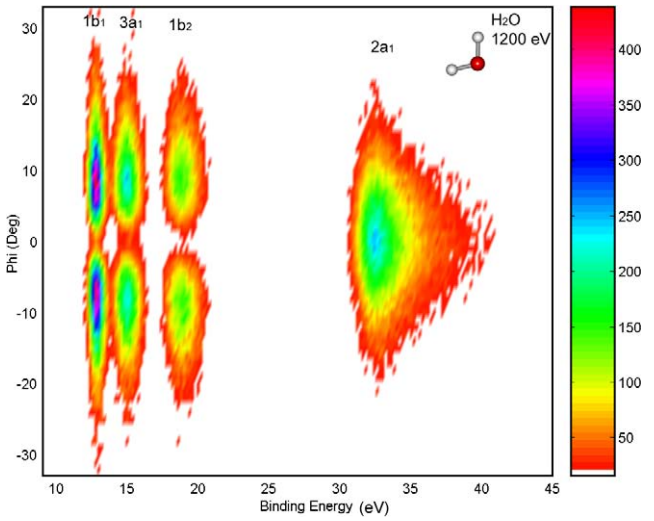

Fig. 1. Valence momentum-energy density distribution of water.

energy. In this map, the three outermost one-electron ionization states relating to the $1b_1$, $3a_1$, $1b_2$ orbitals are clearly resolved and appear as sharp peaks characterized by a p-type electron momentum distribution, which is qualitatively in line with the presence of one nodal plane in the corresponding canonical orbitals. For each of these three states, this profile implies thus a vanishing (e, 2e) ionization intensity at momentum origin, and goes through a maximum at a non-vanishing electron momentum (or azimuthal angle). In contrast, the ionization band derived from the inner-valence $2a_1$ orbital extends over almost 10 eV at $\phi = 0°$, and exhibits maximal (e, 2e) ionization intensities at the origin of momentum space. The corresponding momentum distribution therefore indicates an s-type canonical orbital, which consistently reflects the lack of a nodal plane.

Electron binding energy spectra can be inferred from this density map for each azimuthal angle defining the momentum of the ionized electron prior to ionization. Inversely, the angular dependence of ionization intensities can be used to reconstruct the experimental electron momentum distributions associated to specific ionization channels.

4.2. Electron binding energy spectra

Fig. 2 shows the (e, 2e) ionization spectrum of H_2O at electron binding energies ranging from 9 to 45 eV and at an impact energy of 1200 eV plus binding energies. This spectrum was obtained by integrating the electron density map of Fig. 1 over all azimuthal angles. Gaussian functions have been fitted to the most important bands in this spectrum, using vertical ionization potentials and Franck–Condon widths (folded with the EMS instrument energy resolution 0.68 eV FWHM) estimated from photoelectron spectroscopy measurements [80]. The relative energy spacings of the Gaussian peaks were estimated from experimental estimates for the vertical ionization potentials, with small adjustments to compensate the asymmetries in the shape of the Franck–Condon envelopes. The absolute binding energy scale was set by assigning the energy of the $1b_1$ peak to the vertical ionization potential, as measured by high resolution PES [80]. The centers and widths of these Gaussian bands are listed in Table 1. The simulations displayed in Fig. 2 were obtained by convoluting the contributions from each identified ionization line by a Gaussian spread function with a width fitted to the EMS experiment, and by scaling line intensities proportionally to the computed ADC(3) pole strengths. Magnification of the experimental (e, 2e) ionization spectrum reveals a shallow peak at ~27.1 eV, which defines the shake-up onset for the $2a_1$ orbital. This peak is certainly not ascribable to a shake-off band, the double ionization threshold being located at 41.3 eV, according to benchmark CCSD(T)/raTZ calculations. At the same level, the one-electron vertical ionization threshold related to the $1b_1$ orbital lies at 12.67 eV.

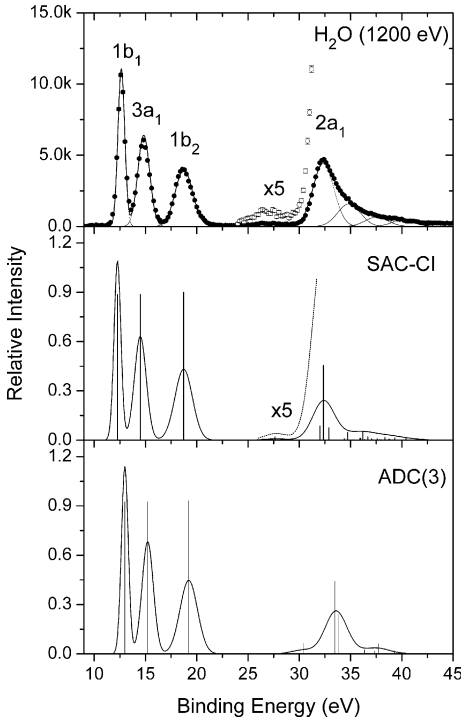

Fig. 2. Experimental binding energy spectrum summed over all ϕ angles (top) compared with SAC-CI (middle) and ADC(3) (bottom) theoretical simulations. See text for details.

Agreement between theory and experiment for the outer-valence bands at electron binding energies below 20 eV is quantitatively satisfactory enough (~0.3 eV accuracy). The ADC(3) vertical one-electron binding energies slightly overestimate the experimental ones by ~0.4 eV, whereas SAC-CI underestimate the experimental values by ~0.3 eV. All the reported theoretical calculations (Fig. 2, Table 1) indicate a partial breakdown of the orbital picture of ionization for the innermost $2a_1$ orbital, in the form of a dispersion of the ionization intensity into shake-up lines ranging from 30 to 40 eV around one main line ($\Gamma > 0.4$) at ~33 eV, which explains the $2a_1$ intensity spreading over almost 10 eV in the experimental spectrum. In this electron binding energy region, the ADC(3) results for shake-up ionization energies are at the best qualitative with respect to the distribution of intensity, due to the limitation of the excitation subspace to the manifold of singly-excited 2h-1p states in the radical cation, and treatment therefore of the 2h-1p states at first-order only in the correlation potential. Whatever the employed basis set, the ADC(3) calculations locate the $2a_1$ shake-up onset at ~30.2 to ~30.4 eV, thus at 3 eV above experiment. In contrast, the SAC-CI calculations locate this threshold at ~27.6 eV, thus in almost perfect agreement with experiment. One cannot entirely rule out the possibility that the employed block-Davidson diagonalization approach was not powerful enough for recovering at the ADC(3)/raTZ level Rydberg-like shake-up ionization lines with

Table 1
Ionization energies (IE, in eV), experimental band widths (FWHM, in eV) and spectroscopic intensities (or pole strengths, PS) for H_2O

	EMS		SAC-CI			ADC(3)		
	IE (FWHM)	PS[a]	IE	PS	State	IE	PS	MO assignment
$1b_1$	12.6(0.78)	1.00	12.272	0.888	$^2B_1$	12.990	0.925	$1b_1$
$3a_1$	14.8(1.35)	1.00	14.496	0.888	$^2A_1$	15.214	0.925	$3a_1$
$1b_2$	18.7(2.0)	1.00	18.723	0.900	$^2B_2$	19.217	0.932	$1b_2$
$2a_1$	27.1(2.6)	0.021	27.641	0.020	$^2A_1$	30.388	0.065	$2a_1$
			27.932	0.001	$^2B_1$			
			29.269	0.002	$^2B_1$			
			29.694	0.001	$^2B_2$			
			32.013	0.086	$^2A_1$			
			32.244	0.001	$^2B_1$	32.028	0.001	$1b_1$
$2a_1$	32.4(2.4)	0.495	32.357	0.455	$^2A_1$	33.469	0.440	$2a_1$
			32.712	0.002	$^2B_1$			
			32.898	0.076	$^2A_1$			
			33.229	0.001	$^2B_2$			
			33.444	0.001	$^2B_1$			
			34.216	0.001	$^2B_2$			
$2a_1$	34.8(2.6)	0.186	34.377	0.008	$^2A_1$	33.864	0.239	$2a_1$
			34.717	0.048	$^2A_1$			
			34.864	0.000	$^2B_2$			
			35.101	0.001	$^2B_1$			
			35.224	0.003	$^2A_1$			
			35.560	0.002	$^2B_1$			
			35.912	0.011	$^2A_1$			
			35.981	0.012	$^2B_1$			
			36.175	0.001	$^2B_1$			
$2a_1$	37.5(2.6)	0.072	36.177	0.049	$^2A_1$	36.369	0.024	$2a_1$
			36.382	0.004	$^2A_1$	36.859	0.004	$2a_1$
			36.569	0.002	$^2B_2$			
			36.691	0.021	$^2A_1$	37.339	0.018	$2a_1$
			37.055	0.008	$^2A_1$	37.726	0.062	$2a_1$
			37.113	0.004	$^2B_1$			
			37.203	0.001	$^2B_1$			
			37.596	0.009	$^2A_1$			
			37.812	0.003	$^2B_1$			
			37.888	0.003	$^2B_2$			
			37.909	0.001	$^2B_1$			
			38.005	0.003	$^2B_1$			
			38.098	0.002	$^2A_1$			
			38.346	0.017	$^2A_1$			
			38.686	0.001	$^2B_1$			
			38.720	0.005	$^2A_1$			
			38.728	0.004	$^2B_2$			
			38.767	0.001	$^2B_1$			
			38.820	0.006	$^2A_1$			
			38.896	0.002	$^2A_1$			
			38.981	0.002	$^2A_1$			
			39.058	0.003	$^2A_1$			
			39.201	0.001	$^2B_1$			
			39.290	0.001	$^2B_1$			
$2a_1$	40.1(2.6)	0.047	39.321	0.013	$^2A_1$	39.307	0.010	$2a_1$
			39.524	0.001	$^2A_1$			
			40.227	0.001	$^2A_1$			
			40.342	0.001	$^2B_1$			
			40.393	0.012	$^2A_1$			
			40.839	0.001	$^2A_1$			
			41.066	0.001	$^2A_1$			
			41.517	0.006	$^2A_1$			

[a] The intensity rescaling relative to the $1b_2$ orbital implies an experimental pole strength equal to one for the $1b_2^{-1}$ ionization line. Note that on theoretical side, the pole strength is necessarily smaller than 1, except for a modelling of ionization processes at first-order in correlation (Koopmans' theorem).

particularly low spectroscopic strengths, lower than the considered threshold ($\Gamma < 0.001$). Nonetheless, it is in our opinion unlikely that extending further the exploration of the shake-up bands in the ADC(3) spectrum will improve

the agreement with experiment in this energy region, because, according to all calculations, the shake-up onset in the ionization spectrum of water relates to an excited electronic state of the radical cation that is strongly dominated by $x a_1^+ \, 1b_1^{-2}$ contributions. Using the time-dependent picture underlying one-particle Green's Function theory and the Feynman diagrams recovered in an ADC(3) scheme by the dynamic component of the self-energy (see Fig. 1 in Ref. [54] and references therein), these states can be regarded as deriving from the diffusion of a strongly localized and almost atomic-like (O_{2s}^{-1}) $2a_1^{-1}$ electron hole vacancy into the $1b_1$ (O_{2p} lone pair) orbital, along with a single electronic excitation from the same lone pair orbital into a very diffuse unoccupied xa_1 orbital (Fig. 3). In view of the involved charge transfers, the states at the shake-up onset of water are therefore certainly subject to considerable electronic relaxation effects, hence their location at a much lower electron binding energy than the $2a_1^{-1}$ main line. Remembering that at the ADC(3) level the shake-up states are described through first-order only in the correlation potential, the corresponding electron binding energies must therefore be very much sensitive to the inclusion of higher-order (3h-2p, 4h-3p, etc.) electronic excitations in the shake-up manifold, which most certainly explain the highly significant difference of ~2.7 eV between the ADC(3) and SAC-CI results. In contrast, weaker electronic relaxation effects are expected for the most intense $2a_1$ lines, at 33.5 eV ($\Gamma = 0.44$) and 33.9 eV ($\Gamma = 0.24$) in the ADC(3) spectrum, because of their more pronounced 1 h character. Indeed, these lines can be correlated with an intense satellite ($\Gamma = 0.46$) at 32.4 eV in the SAC-CI spectrum, hence a shift of 1.5 ± 0.2 eV only. At the ADC(3)/raTZ and SAC-CI general R/raTZ levels, the location of the most intense shake-up bands are thus reproduced within an accuracy of ~1 eV and ~0.2 eV, respectively.

The shift of ~2.7 eV from the ADC(3) to the SAC-CI spectrum for the $x a_1^+ \, 1b_1^{-2}$ shake-up onset of water is thus most certainly ascribable to its greatest extent to the dynamical correlation and relaxation effects described by double and higher-order electronic excitations in the radical cation. Indeed, further CIS and CIS(D) calculations of the excitation energies of the water radical cation employing the aug-cc-pVTZ indicate a shift of the shake-up $2a_1$ excitation onset towards lower energies by 1–1.5 eV when double electronic excitations are included. In order to assess more in details the role of multiple electronic excitations on the location of the $2a_1$ shake-up onset, we display in Table 2 estimates of ionization energies that were obtained by adding to the experimental value (12.62 eV) [81] for the first ionization energy of water the excitation energies computed at the MR-SDCI or MR-RSPT2/3 levels for the water radical cation in its $^2B_1$ ground state. The role of the basis set in these calculations is investigated in details. Whatever the employed basis set, these calculations locate the $2a_1$ shake-up onset at electron binding energies ranging from 27.1 to 27.4 eV, thus in quantitative agreement with experiment. The same procedure applied to the best MR-SDCI/raTZ results for excitation energies in H_2O^+ locates the $1a_1$ and $1b_2$ ionization lines at 14.87 eV and 19.00 eV, to compare with experimental values of 14.8 and 18.7 eV, respectively. With this indirect approach for estimating electron binding energies, pole strengths are unfortunately not readily accessible.

4.3. Momentum distribution

Fig. 4 shows the experimental momentum distributions for the outer valence orbitals of H_2O compared with the results of our theoretical calculations. In the present work, the theoretical spherically averaged momentum distributions have been convoluted with the experimental momentum resolution using Monte Carlo methods [82]. The CI theoretical curves are taken from Ref. [56], and convolved according to our experimental momentum resolution. The experimental momentum distributions associated to all ionization bands in a (e, 2e) spectrum are most commonly rescaled using a global renormalization factor enabling the best fit with theory for one carefully selected ionization band, assuming that the theoretical momentum distribution $\rho(p)$ associated to this reference is normalized via

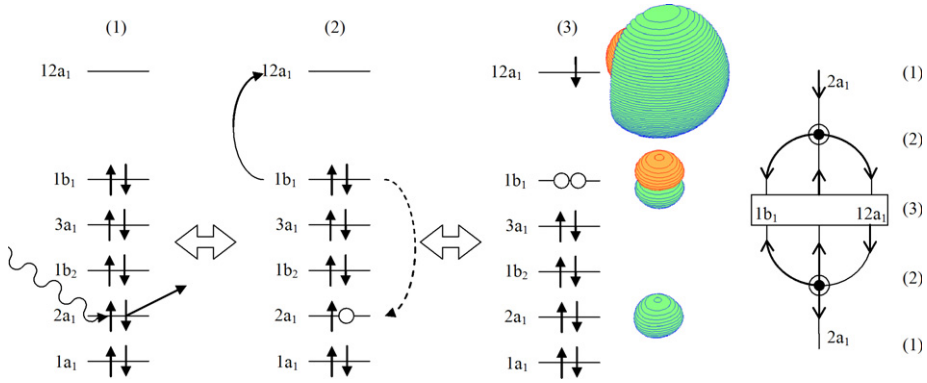

Fig. 3. Electronic excitation processes involved in the shake-up onset of water, along with a time-dependent interpretation of the electronic interactions leading to this state using the one-hole ADC(3) dynamic self-energy diagram (see Fig. 1 in Ref. [54] for a complete diagrammatic expansion of this component of the self-energy). The displayed molecular orbitals were drawn using Molden 4.3, using the same edge size (25.5 bohr) and density contour value (0.01).

Table 2
Multi-reference calculations of the ionization energies of water

State	MR-RSPT2/cc-pVDZ	MR-RSPT2/cc-pVTZ	MR-RSPT2/aug-cc-pVDZ	MR-RSPT2/rTZ	MR-RSPT3/cc-pVDZ	MR-RSPT3/cc-pVTZ	MR-RSPT3/aug-cc-pVDZ	MR-SDCI/cc-pVDZ	MR-SDCI/cc-pVTZ	MR-SDCI/aug-cc-pVDZ	MR-SDCI/rTZ
$^2B_2$	33.04	32.82	32.80	33.48	33.13	32.96	33.13	33.14	32.93	32.89	32.87
$^2A_1$	33.05	32.37	32.05	33.32	33.22	33.00	32.91	33.14	32.78	32.84	32.62
$^2B_1$	32.69	32.33	32.46	32.50	32.93	33.07	32.48	32.86	32.67	31.92	31.84
$^2A_1$	32.07	31.94	31.94	32.00	32.11	32.00	32.08	32.04	31.95	31.89	32.12
$^2B_2$	29.34	29.17	29.28	33.81	29.48	29.44	30.16	29.47	29.37	29.32	29.32
$^2B_1$	28.90	28.81	28.83	28.87	28.94	28.88	28.87	28.93	28.84	28.79	28.80
$^2B_1$	27.26	27.21	27.10	27.20	27.30	27.28	27.14	27.29	27.26	27.09	27.18
$^2A_1$	27.17	27.18	27.13	27.19	27.24	27.27	27.21	27.18	27.23	27.16	27.41
$^2B_2$	19.13	18.94	19.04	18.95	19.17	18.99	19.08	19.21	19.03	19.09	19.00
$^2A_1$	14.88	14.81	14.86	14.81	14.91	14.83	14.89	14.88	14.87	14.91	14.87
$^2B_1$	12.62	12.62	12.62	12.62	12.62	12.62	12.62	12.62	12.62	12.62	12.62

$4\pi \int_0^\infty \rho(p)p^2 dp = 1$. The theoretical calculations for the $1b_2$ orbital with HF, DFT, ADC(3) and CI methods all give almost the same momentum distributions. Following the procedure by Bawagan et al. [31], the ionization band taken in this work as the reference for intensity rescaling was therefore the $1b_2$ orbital, assuming an experimental spectroscopic pole strength equal to 1 for the related one-electron transition. For this orbital, the agreement between theory and experiment is truly optimal throughout the investigated range of electron momenta, except at momenta below 0.2 a.u. where a slight but clearly discernible rise of the measured electron density may reflect a symmetry breaking that is possibly ascribable to vibrational effects [83]. This slight discrepancy between experimental distributions and theoretical calculations for the $1b_2$ orbital is also possibly due to distorted wave effects. Indeed, a comparison of Figs. 4 and 5 demonstrates that this discrepancy almost vanishes at an impact energy of 2400 eV plus binding energies. The shape and spread of the momentum distributions derived from the other bands remain on the contrary unaffected by an increase of the kinetic energy of the impinging electron.

In general, theoretical calculations reliably reproduce the measured momentum distribution, except when a very limited basis set such as 6-31G is employed [73]. Even with a basis set as large as the aug-cc-pVTZ one, the HF calculations rather obviously fail to quantitatively reproduce the $1b_1$ and $3a_1$ experimental momentum distributions. In contrast, the agreement with the experimental curves is much better with this basis set when using B3LYP Kohn–Sham

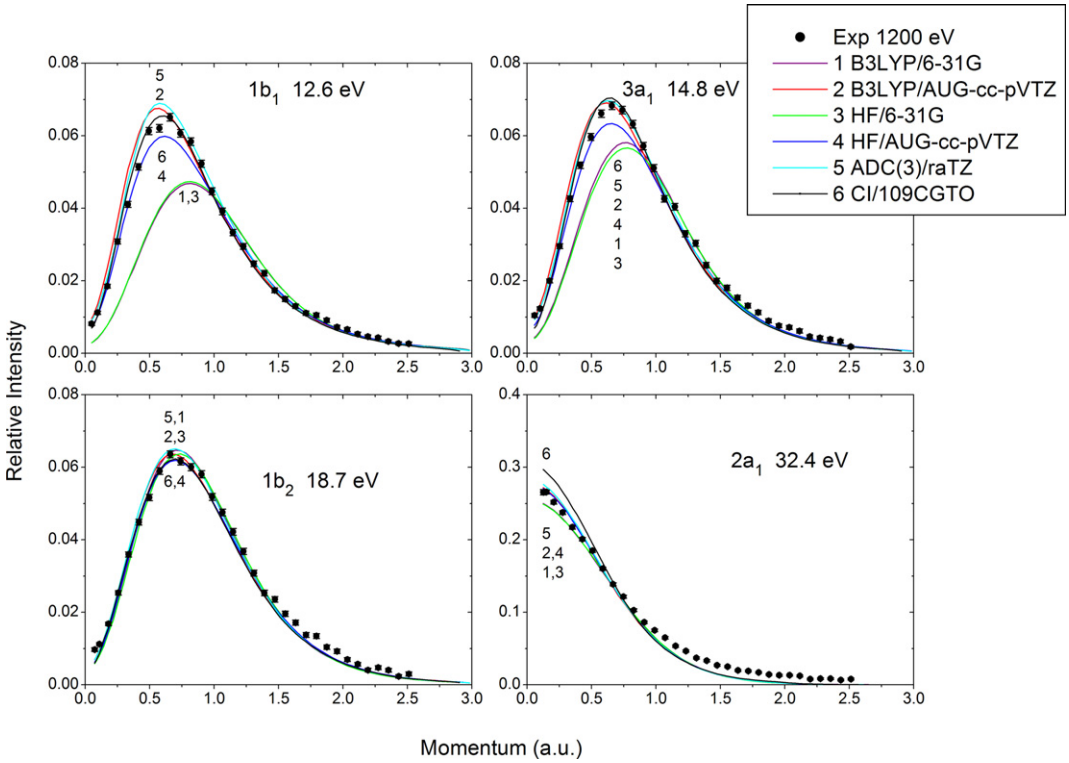

Fig. 4. Convolved and spherically averaged momentum distributions of the $1b_1$, $3a_1$, $1b_2$, $2a_1$ orbitals at an impact energy of 1200 eV plus binding energy.

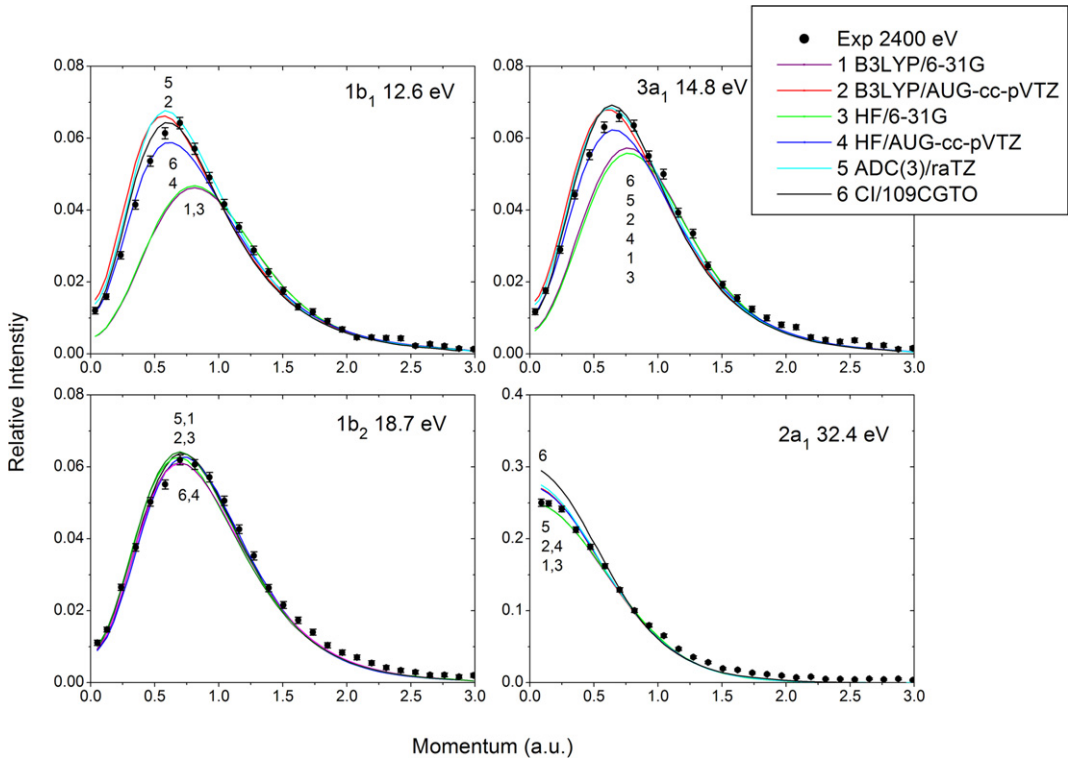

Fig. 5. Convolved and spherically averaged momentum distributions of the $1b_1$, $3a_1$, $1b_2$, $2a_1$ orbitals at an impact energy of 2400 eV plus binding energy.

orbitals, or Dyson orbitals derived from CI or ADC(3) calculations. The latter theoretical orbital momentum distributions are found again to almost coincide.

The experimental momentum distribution inferred in Fig. 4 from an angular analysis of the (e, 2e) ionization intensity ascribed to the peak at 32.4 eV is compared in Fig. 4 with the Dyson orbital momentum distribution characterizing the closest shake-up line in the ADC(3) spectrum, namely the satellite line at 33.5 eV with a pole strength of 0.44. All theoretical distributions for this orbital are normalized. It appears that the CI/109GTO's calculations by Bawagan et al. [31] slightly overestimate the $2a_1$ orbital density that is experimentally observed at low momenta.

The experimental momentum distribution of the satellite peak at 27.1 eV is compared with DFT calculations at the B3LYP/aug-cc-pVTZ level for the $2a_1$ momentum distribution in Fig. 6. A slight difference between the theoretical curves for the momentum densities computed at an impact energy of 1200 eV (dashed line) and 2400 eV (solid line) is simply due to convolutions with slightly different momentum resolutions. The estimated experimental pole strength for this band amounts to 0.021 at both impact energies. The shape of the experimental distribution compared with the theoretical one confirms the relationship of this shake-up band with the $2a_1$ orbital, in agreement with the theoretical SAC-CI, MR-SDCI or MR-RSPT2/3 calculations described in the previous section, or assignment by Ehara et al. [53].

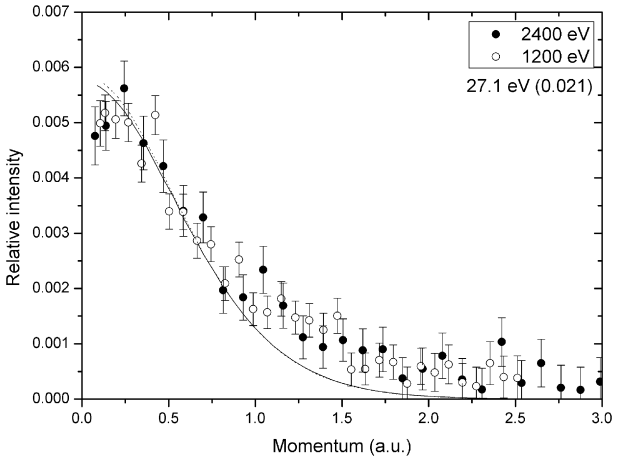

Fig. 6. Convolved and spherically averaged momentum distribution inferred for the shake-up peak at 27.1 eV at impact energies of 1200 eV and 2400 eV plus binding energy.

It thus experimentally appears that the intensity of the $2a_1$ shake-up onset at 27.1 eV does not show any dynamical dependence on the impact energy, at kinetic energies above 1200 eV. In contrast, it is interesting to note that in synchrotron experiments the intensity of this band was found to vary in a remarkable way with the photon energy [52]. One obvious explanation is that with photoelectron experiments at photon energies of 100 eV, residual interactions between the molecular radical cation and the outgoing electron remain strong, which results in severe alterations of

the continuum wave function, the shape of which is strongly dependent on the kinetic energy of the ionized electron. This is not the case with ionization events induced by electron impact at high kinetic energies: under the so-called EMS conditions, the impinging and outgoing electrons are on the contrary reliably described by plane waves.

4.4. Basis set effects

Fig. 7 confirms the rather strong influence of the basis set on the theoretical momentum distributions associated to the $1b_1$ and $3a_1$ orbitals. Although Bawagan et al. have discussed these effects [31], it is still instructive, with regards to software and hardware developments over the last 20 years, to investigate further the influence of the basis. The original HEMS program developed at the University of British Columbia (UBC) [31], which is now widely used to calculate electron momentum distributions, cannot handle basis sets containing *g*-type polarization functions and beyond. A new program for computing momentum distributions was therefore developed for this purpose at Tsinghua University. This program, named NEMS, was coded using FORTRAN90. It makes use of general analytic formula [84] for handling basis functions, whatever their angular momentum quantum number. The fast algorithm of continual fractions [85] was used for numerically computing spherical Bessel functions $j_l(x)$. This algorithm is considered to be the best strategy for calculating high order

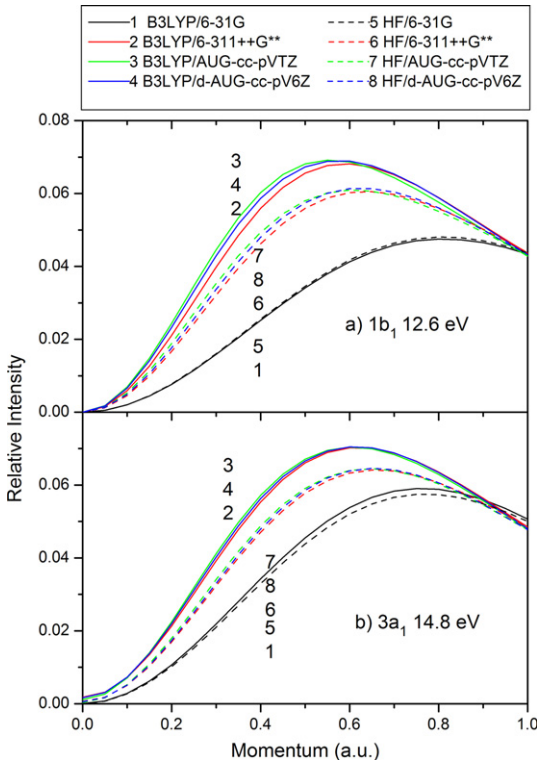

Fig. 7. Momentum distributions of (a) $1b_1$ orbital and (b) $3a_1$ orbital at various theoretical levels (the experimental resolution is not accounted for).

Table 3
Basis-set dependence of the total energy and dipole moment of H_2O

Method/basis set	Size	Dipole moment (*D*)	Total energy (Hartree)
B3LYP/6-31G	13	2.463	−76.3849
B3LYP/6-311++G**	37	2.1625	−76.4592
B3LYP/aug-cc-pVTZ	105	1.8409	−76.4671
B3LYP/d-aug-cc-pV6Z	551	1.8548	−76.4742
HF/6-31G	13	2.6299	−75.9834
HF/6-311++G**	37	2.2392	−76.0529
HF/aug-cc-pVTZ	105	1.9757	−76.0611
HF/d-aug-cc-pV6Z	551	1.9815	−76.0674
Experimental		1.8546 ± 0.0006[a]	76.4376 ± 0.0004[b]

[a] Ref. [85].
[b] Refs. [87,31]. The value reported here is the non-relativistic, non-vibrating total energy of water.

spherical Bessel functions $j_l(x)$ near space origin ($x \sim 0$) and in the asymptotic region ($x \gg 1$). This new program enabled us to compute momentum distributions using a much larger basis set (d-aug-cc-pV6Z), which includes *g*-, *h*-, and *i*-type basis functions.

Table 3 gives the calculated dipole moment and total energy of water molecule using HF and DFT methods with various basis sets. The slight difference in total energies, as well as in dipole moments, between the aug-cc-pVTZ and d-aug-cc-pV6Z basis sets indicates that these basic ground state properties, and the underlying wavefunction therefore, are almost effectively converged with the aug-cc-pVTZ basis set. The excellent agreement between our best theoretical (B3LYP/d-aug-cc-pV6Z) values and the experimentally inferred results [86,87] for the dipole moment and total energy (Table 3), as well as for the electron momentum distributions (Figs. 4 and 5), confirms that DFT calculations incorporating ground state correlation effects are superior to the HF approach for studying molecular properties related to the ground state electron density. Note nonetheless that DFT is semi-empirical in nature, and does not obey therefore the variational principle regarding the total energy. Indeed, in this case, it is found that close to the limit of a complete basis set, the B3LYP total energy is obviously lower than the experimental value found for the total non-relativistic energy at equilibrium [31]. It is thus here worth remembering that the electron densities measured in EMS relate to transition amplitudes between the neutral ground state and cationic states – they do not therefore simply relate to ground state electron densities for specific sets of orbitals.

As is clearly seen from Fig. 7, the momentum distribution computed for the $1b_1$ orbital at low electron momenta tends to increase with the number of diffuse functions in the basis sets (see the progression of curves 1–3 for DFT, and 5–7 for HF). Beyond the aug-cc-pVTZ basis set, a slight reversal in this trend is seen when considering the results obtained with the largest basis set considered in this study, namely d-aug-cc-pV6Z (see curves 4 and 8). It is interesting to note that, in the saturation limit, the same trends are observed both with GTO and STO basis sets [31]. There-

fore, this variation in the influence of the basis set might be due to the fact that the d-aug-cc-pV6Z basis set contains more split-valence components. All the theoretical momentum distributions are generated using the newly developed NEMS program, which can handle any type of atomic basic functions.

5. Conclusions

In this paper, we report the results of an exhaustive reinvestigation, throughout the valence region, of the electronic structure of water using a new (e, 2e) spectrometer, which enables a much improved energy resolution of $\Delta E = 0.68$ eV, as well as azimuthal and polar angle resolutions of $\Delta\phi = \pm 0.84°$ and $\Delta\theta = \pm 0.53°$, respectively. The measured electron impact (e, 2e) ionization spectra were compared with a variety of calculations of one-electron and shake-up ionization spectra employing the 1p-GF/ADC(3) and SAC-CI general approaches, and of excitation energies in the water radical cation employing multi-reference theories (MR-SDCI, MR-RSPT2, MR-RSPT3). Highly accurate experimental momentum distributions derived from an angular analysis of (e, 2e) ionization intensities were compared with spherically averaged momentum distributions derived from HF orbitals, B3LYP Kohn–Sham orbitals, and ADC(3) Dyson orbitals. In view of a very significant failure of the target HF approximation for the $1b_1$ and $3a_1$ orbitals, these improved momentum distributions sheld light again on the importance of electronic correlation in quantitative theoretical studies of electronic densities. A weakly discernible peak at 27.1 eV defining the experimental shake-up onset of water was confirmed to relate to a complex set of shake-up states produced by ionization of the $2a_1$ orbital. The influence of Rydberg-type basis functions on the energies of these states is rather limited. On the other hand, and probably because of the atomic-like (O_{2s}) nature of the involved orbital, the $2a_1$ shake-up onset is associated to particularly pronounced charge transfer processes towards the continuum resulting in unusually strong electronic relaxation effects. It is therefore strongly dependent on the inclusion of double electronic excitations in the shake-up excitation operator manifold. ADC(4) calculations incorporating 3h-2p shake-up states and 3p-2h shake-on states in this manifold would therefore be very much needed for reproducing accurately enough the lowest shake-up bands of water within the framework of one-particle Green's Function theory.

A new algorithm has been developed for calculating electron momentum distributions using almost complete basis sets, such as d-aug-cc-pV6Z. A comparison with results obtained with smaller basis sets indicate near saturation at the HF/aug-cc-pVTZ and B3LYP/aug-cc-pVTZ levels.

Acknowledgements

This work is supported by the National Natural Science Foundation of China under Contract No. 10575062 and Specialized Research Fund for the Doctoral Program of Higher Education under 20050003084. The authors also acknowledge the financial support by the *Fonds voor Wetenschappelijk Onderzoek-Vlaanderen* (FWO) and the *Bijzonder OnderzoeksFonds* (BOF) of the Hasselt University. Yanru Huang has been working nine months (15th June 2006–14th March 2007) as a PhD student at Hasselt University, thanks to a fellowship obtained within the framework of a bilateral program for scientific cooperation between Belgium (Flanders) and PR China. Balazs Hajgato was post-doctoral researcher at Hasselt University from 01st July to 31st December 2006. He acknowledges further financial support from the Technical University of Budapest, Hungary, from 1st February to 30th April 2007, and from a DFT-network sponsored by the FWO-Vlaanderen (Belgium), from 1st May 2007 to 30th April 2008.

References

[1] I.E. McCarthy, E. Weigold, Rep. Prog. Phys. 91 (1991) 789.
[2] E. Weigold, I.E. McCarthy, Electron Momentum Spectroscopy, Kulwer/Plenum, New York, 1999.
[3] C.E. Brion, Int. J. Quantum Chem. 29 (1986) 397.
[4] M.A. Coplan, J.H. Moore, J.P. Doering, Rev. Mod. Phys. 66 (1994) 985.
[5] R. McWeeny, B.T. Pickup, Rep. Prog. Phys. 43 (1980) 1065.
[6] Y. Ohrn, G. Born, Adv. Quantum Chem. 13 (1981) 1.
[7] B.T. Pickup, Chem. Phys. 19 (1977) 93.
[8] G.M. Seabra, I.G. Kaplan, V.G. Zakrzewski, J.V. Ortiz, J. Chem. Phys. 121 (2004) 142.
[9] M.S. Deleuze, S. Knippenberg, J. Chem. Phys. 125 (2006) 104309.
[10] Y.R. Huang, S. Knippenberg, B. Hajgato, J.-P. Francois, J.K. Deng, M.S. Deleuze, J. Phys. Chem. A 111 (2007) 5879.
[11] C.G. Ning, X.G. Ren, J.K. Deng, G.L. Su, S.F. Zhang, S. Knippenberg, M.S. Deleuze, Chem. Phys. Lett. 421 (2006) 52.
[12] M.S. Deleuze, B.T. Pickup, J. Delhalle, Mol. Phys. 83 (1994) 655.
[13] H. Hafied, A. Eschenbrenner, C. Champion, M.F. Ruiz-López, C. Dal Cappello, I. Charpentier, P.A. Hervieux, Chem. Phys. Lett. 439 (2007) 55.
[14] R.H. Page, R.J. Larkin, Y.R. Yhen, Y.T. Lee, J. Chem. Phys. 88 (1987) 2249.
[15] J.E. Reutt, L.S. Wang, Y.T. Lee, D.A. Shirley, J. Chem. Phys. 85 (1986) 6928.
[16] D. Lefaivre, P. Marmet, Can. J. Phys. 56 (1978) 1549.
[17] R. Botter, J. Carlier, J. Electron Spectrosc. Relat. Phenom. 12 (1977) 55.
[18] R.N. Dixon, G. Duxbury, J.W. Rabalais, L. Asbrink, Mol. Phys. 31 (1976) 423.
[19] L. Karlsson, L. Mattson, R. Jadrny, R.G. Albridge, S. Pinchas, T. Bergmark, K. Siegbahn, J. Chem. Phys. 62 (1975) 4745.
[20] T.P. Debies, J.W. Rabalais, J. Am. Chem. Soc. 97 (1975) 487.
[21] J.W. Rabalais, T.P. Debies, J.L. Berkosky, J.-T.J. Huang, F.O. Ellison, J. Chem. Phys. 61 (1974) 516.
[22] T. Bermark, L. Karlsson, R. Jadrny, L. Mattsson, R.G. Albridge, K. Siegbahn, J. Electron Spectrosc. Relat. Phenom. 4 (1974) 85.
[23] D.H. Katayama, R.E. Huffman, C.L. O'Bryan, J. Chem. Phys. 59 (1973) 4309.
[24] L. Asbrink, J.W. Rabalais, Chem. Phys. Lett. 12 (1971) 182.
[25] C.R. Brundle, D.W. Turner, Proc. Roy. Soc. (London) A307 (1968) 27.
[26] M.J. Campbell, J. Liesegang, J.D. Riley, R.C.G. Leckey, J.G. Jenkin, R.T. Poole, J. Electron Spectrosc. Relat. Phenom. 15 (1979) 83.
[27] K.E. McCulloh, Int. J. Mass Spectrom. Ion. Phys. 21 (1976) 333.

[28] A.J. Dixon, S. Dey, I.E. McCharthy, E. Weigold, G.R. Williams, Chem. Phys. 21 (1977) 81.
[29] S.T. Hood, A. Hamnett, C.E. Brion, J. Electron Spectrosc. Relat. Phenom. 11 (1977) 205.
[30] A.O. Bawagan, L.Y. Lee, K.T. Leung, C.E. Brion, Chem. Phys. 99 (1985) 367.
[31] A.O. Bawagan, C.E. Brion, E.R. Davison, D. Feller, Chem. Phys. 113 (1987) 19.
[32] L.S. Cederbaum, Mol. Phys. 28 (1974) 479.
[33] K. Siegbahn, C. Nordling, G. Johansson, J. Hedman, P.F. Heden, K. Hamrin, U. gelius, T. Berkmark, L.O. Werme, R. Manne, Y. Baer, ESCA Applied to Free Molecules, North-Holland, Amsterdam, 1969.
[34] B.T. Pickup, O. Goscinski, Mol. Phys. 26 (1973) 1013.
[35] D.P. Chong, F.G. Herring, D. Mc Williams, J. Chem. Phys. 61 (1974) 3567.
[36] P. Jörgensen, J. Simons, J. Chem. Phys. 63 (1975) 5302.
[37] E.R. Davidson, J. Comput. Phys. 17 (1975) 87.
[38] I. Hubac, M. Urban, Theor. Chim. Acta 45 (1977) 195.
[39] W. von Niessen, G.H.F. Diercksen, L.S. Cederbaum, J. Chem. Phys. 67 (1977) 4124.
[40] M.F. Hermann, D.L. Yeager, K.F. Freed, Chem. Phys. 29 (1978) 77.
[41] V. Carravetta, R. Moccia, Mol. Phys. 35 (1978) 129.
[42] H.A. Kurtz, Y. Öhrn, J. Chem. Phys. 69 (1978) 1162.
[43] G. Born, Y. Öhrn, Phys. Scripta 21 (1980) 378.
[44] I. Cacelli, R. Moccia, V. Carravetta, Chem. Phys. 71 (1982) 199.
[45] J. Baker, B.T. Pickup, Mol. Phys. 49 (1983) 651.
[46] J. Baker, Chem. Phys. 79 (1983) 117.
[47] J.V. Ortiz, R. Basu, Y. Öhrn, Chem. Phys. Lett. 103 (1983) 29.
[48] D.L. Yeager, J. Chem. Phys. 105 (1996) 170.
[49] D. Heryadi, D.L. Yeager, J.T. Golab, J.A. Nichols, Theor. Chim. Acta 90 (1995) 273.
[50] M. Nooijen, J.G. Snijders, Int. J. Quantum Chem. 48 (1993) 15.
[51] R.C. Morrison, G.H. Liu, J. Comp. Chem. 13 (1992) 1004.
[52] M.S. Banna, B.H. McQuaide, R. Malutzki, V. Schmidt, J. Chem. Phys. 84 (1986) 4739.
[53] M. Ehara, M. Ishida, Nakatsuji, J. Chem. Phys. 114 (2001) 8990.
[54] M.S. Deleuze, M.G. Giuffreda, J.-P. François, L.S. Cederbaum, J. Chem. Phys. 111 (1999) 5851.
[55] Y. Zheng, C.E. Brion, M.J. Brunger, K. Zhao, A.M. Grisogono, S. Braidwood, E. Weigold, S.J. Chakravorty, E.R. Davidson, A. Sgamellotti, W. von Niessen, Chem. Phys. 212 (1996) 269.
[56] P. Duffy, D.P. Chong, M.E. Casida, D.R. Salahub, Phys. Rev. A 50 (1994) 4704.
[57] C. Lee, W. Yang, R.G. Parr, Phys. Rev. B 37 (1988) 785.
[58] This basis set was obtained from the Extensible Computational Chemistry Environment Basis Set Database, Version 02/02/06, as developed and distributed by the Molecular Science Computing Facility, Environmental and Molecular Sciences Laboratory which is part of the Pacific Northwest Laboratory, and funded by the US Department of Energy. Also see reference: A.K. Wilson, T.V. Mourik, T.H. Dunning Jr., J. Mol. Struct. (THEOCHEM) 388 (1997) 339.
[59] L.S. Cederbaum, W. Domcke, Adv. Chem. Phys. 36 (1977) 205.
[60] J. Schirmer, L.S. Cederbaum, O. Walter, Phys. Rev. A 28 (1983) 1237.
[61] J. Schirmer, G. Angonoa, J. Chem. Phys. 91 (1989) 1754.
[62] H.G. Weikert, H.-D. Meyer, L.S. Cederbaum, F. Tarantelli, J. Chem. Phys. 104 (1996) 7122.
[63] S. Knippenberg, K.L. Nixon, H. Mackenzie-Ross, M.J. Brunger, F. Wang, M.S. Deleuze, J.-P. François, D.A. Winkler, J. Phys. Chem. A 109 (2005) 9324.
[64] S. Knippenberg, K.L. Nixon, M.J. Brunger, T. Maddern, L. Campbell, N. Trout, F. Wang, W.R. Newell, M.S. Deleuze, J.-P. François, D.A. Winkler, J. Chem. Phys. 121 (2004) 10525.
[65] W. Adcock, M.J. Brunger, I.E. McCarthy, M.T. Michaelewicz, W. von Niessen, F. Wang, D.A. Winkler, J. Am. Chem. Soc. 122 (2000) 3892.
[66] M.S. Deleuze, Int. J. Quantum Chem. 93 (2003) 191.
[67] M.S. Deleuze, J. Phys. Chem. A 108 (2004) 9244.
[68] T.H. Dunning, P.J. Hay Jr., Methods of Electronic Structure Theory, in: H.F. SchaeferIII (Ed.), Plenum, New York, 1977.
[69] H. Nakatsuji, Chem. Phys. Lett. 177 (1991) 331.
[70] M. Ehara, Y. Ohtsuka, H. Nakatsuji, M. Takahashi, Y. Udagawa, J. Chem. Phys. 122 (2005) 234319.
[71] M. Ehara, M. Ishida, H. Nakatsuji, J. Chem. Phys. 117 (2002) 3248.
[72] T.J. Dunning Jr., J. Chem. Phys. 90 (1989) 1007.
[73] M.J. Frisch et al., Gaussian03, revision D02, Gaussian Inc, Pittsburgh, PA, 2003.
[74] H.J. Werner, P.J. Knowles, J. Chem. Phys. 89 (1988) 5803.
[75] P.J. Knowles, H.-J. Werner, Chem. Phys. Lett. 145 (1988) 514.
[76] P.J. Knowles, H.-J. Werner, Theor. Chim. Acta 84 (1992) 95.
[77] H.-J. Werner, Mol. Phys. 89 (1996) 645.
[78] MOLPRO is a package of ab initio programs written by H.-J. Werner and P.J. Knowles, with contributions from R.D. Amos, A. Bernhardsson, A. Berning, P. Celani, D.L. Cooper, M.J.O. Deegan, A.J. Dobbyn, F. Eckert, C. Hampel, G. Hetzer, T. Korona, R. Lindh, A.W. Lloyd, S.J. McNicholas, F.R. Manby, W. Meyer, M.E. Mura, A. Nicklass, P. Palmieri, R. Pitzer, G. Rauhut, M. Schütz, H. Stoll, A.J. Stone, R. Tarroni, and T. Thorsteinsson.
[79] X.G. Ren, C.G. Ning, J.K. Deng, S.F. Zhang, G.L. Su, F. Huang, G.Q. Li, Rev. Sci. Instrum. 76 (2005) 063103.
[80] K. Kimura, S. Katsuwata, Y. Achiba, T. Yamazaki, S. Iwata, Handbook of HeI Photoelectron Spectra of Fundamental Organic Molecules, Halsted Press, New York, 1981.
[81] A.W. Potts, W.C. Price, Proc. R. Soc. Lond. A 326 (1972) 181.
[82] P. Duffy, M.E. Casida, C.E. Brion, D.P. Chong, Chem. Phys. 159 (1992) 347.
[83] B.P. Hollebone, J.J. Neville, Y. Zheng, C.E. Brion, Y. Wang, E.R. Davidson, Chem. Phys. 196 (1996) 13.
[84] R.J. Mathar, Int. J. Quantum Chem. 90 (2002) 227.
[85] W.J. Lentz, Appl. Opt. 15 (1976) 668.
[86] S.A. Clough, Y. Beers, G.P. Klein, L.S. Rothman, J. Chem. Phys. 59 (1973) 2254.
[87] B.J. Rosenberg, I. Shavitt, J. Chem. Phys. 63 (1975) 2162.